Rapports internes du LaMSID

H. AMDRIAMBOLOLONA* – D. BOSSELUT* –
P. MASSIN

Methodology for a numerical simulation of an insertion or a drop of the rod cluster control assembly in a PWR

RI-B3-N°006 2007

*Electricité de France – Recherche et Développement

Laboratoire de Mécanique des Structures Industrielles Durables
UMR EDF-CNRS 2832
EDF R&D
1, Avenue du Général de Gaulle - 92141 CLAMART CEDEX FRANCE

Title :

Methodology for a numerical simulation of an insertion or a drop of the rod cluster control assembly in a PWR.

Authors :

H. Andriambololona [a], D. Bosselut [a], P. Massin [b]

[a] Electricité de France – Research and Development Division

1, avenue du Général de Gaulle, 92141 Clamart – France.

[b] Laboratoire de Mécanique des Structures Industrielles Durables -CNRS-EDF, UMR 2832

1, avenue du Général de Gaulle, 92141 Clamart – France.

Corresponding author :

H. Andriambololona

Electricité de France – Research and Development Division

1, avenue du Général de Gaulle, 92141 Clamart cedex – France.

Phone : + 33 1 47 65 33 38

Fax : + 33 1 47 65 39 78

e-mail address : harinaivo.andriambololona@edf.fr

Abstract

In a pressurized water reactor, the rod cluster control assembly is a system which controls the neutronic activity of the core. It consists of long rods, connected by a spider fixture and a cylindrical system for the control drive mechanism. At its withdrawn position, the activity of the core is maximum, and at its completely inserted position, the activity of the core vanishes. In case of emergency, an effective way to shutdown the reactor is to let it drop under its own weight. An other way to verify the efficiency of the rod cluster control assembly is the insertion test. It consists in inserting the rod into its guides and in checking if the reaction friction force is not high enough to block the movement of the rod cluster control assembly.

We present in this paper a methodology for a numerical simulation of an insertion or a drop of the rod cluster control assembly into its guides (discontinuous and continuous guides, guide thimble). A numerical model is elaborated in which many loads are taken into account : fluid load, gravity and friction force between the rod and the guide. The numerical results are compared to experimental measurements obtained from a full-scale structure. A good agreement between the calculated and the measured data is observed.

The numerical model takes into account the possible deflection of the guide. It shows clearly that the friction force cannot be neglected when the guide is bowed. So one can locate a faulty guiding system by examining the reaction force during the insertion test. Then, the numerical model can help the decider to make his choice among different rod cluster/fuel assembly components.

1 Introduction

In a nuclear pressurised water reactor, rod cluster control assemblies are used to control the neutronic activity of the core. They are composed of many rods, containing neutron absorbing material, which are maintained by a spider and a cylindrical body which represents the control rod drive mechanism. The length of the rod is about 4 m with an outer diameter of about 10 mm. It has to move in a guide with an inner diameter slightly larger than the outer diameter of the rod. The correct alignment of the control rod and the guide thimble is assured by a mechanism system guide, a discontinuous guide and a continuous guide. When the control rod is in its withdrawn position, the activity of the core is maximum. When it is in a completely inserted position, the activity of the core vanishes. This article deals with the mechanical behaviour of the rod cluster, it doesn't evaluate the neutronic activity of the core due to the drop of the rod cluster.

Measurements of the rod drop time are commonly used before each reactor start up. This start up may be prevented if the rod drop time exceeds a threshold value, which is imposed by safety requirements. In addition, the measurement of the insertion resistant forces is an indication of a faulty rod cluster/guide tube component. Simulating numerically the drop of a rod cluster may help designers to optimise the configuration of the components related to the rod or the fuel assembly.

In 1994, Taliyan simulated the rod drop in a pressurized heavy water reactor. The kinematics of the rod were obtained by using the dynamic force balance. He developed an empirical formula for the friction factor in the dashpot, depending on the flow clearance geometry (Taliyan, 1994).

In 2003, Wang simulated the rod drop by considering the rod cluster control assembly as a single degree of freedom system. The kinematics of the drop were obtained by

using the dynamic force balance too. The deflection of the guide was not taken into account. The friction at the dash pot was modelled by introducing a damping coefficient depending on the gap between the rod and the guide and some geometric considerations (Wang, 2003).

Later, Aullo has done some simulations of the rod drop and rod insertion with a C-shaped bowed guide thimble (Aullo, 2004). He estimates the insertion drag force with respect to the deflection of the guide, and uses it as an external force depending on the altitude of the rod during the drop. The rod drop simulation is also obtained with a single degree of freedom system and by using the dynamic force balance.

The originality of our study is the consideration of the friction between the guide and the rod in a rather complete finite element model of the components. The objective of the calculations is to help the decider with the choice of the component, and to diagnose the cause of an abnormal rod drop time, or an incomplete rod cluster insertion.

2 Analytical formulation of the problem

Rod drop time is estimated by considering the mechanical and fluid loads. After discretisation by using the finite element approach, the movement of the rod cluster and the guiding system is governed by the following equation :

$$M\ddot{u} + Ku = F_{Gravity} + F_{Friction} + F_{Archimedes} + F_{Guide} + F_{Mechanism} + F_{Stick} \quad (1)$$

Where u is the displacement field, M and K represent the mass and the stiffness matrices.

$F_{Gravity}$ and $F_{Friction}$ are mechanical loads. $F_{Archimedes}$, F_{Guide}, $F_{Mechanism}$ and F_{Stick} are fluid loads. More details about these loads are presented in the next chapters.

2.1 Formulation of the mechanical load

The main mechanical loads are gravity ($F_{Gravity}$) and friction forces ($F_{Friction}$). The contact between the rod and the guide can be characterised by an unilateral contact relation. It can be formulated as no interpenetration between the two previous components. The two components are separated or act on each other. The geometry of the structure is re-actualised at each time step.

The resolution of the contact-friction problem is treated on the discretised numerical model with a master/slave method, so that the node of the slave component cannot penetrate into the master component. Contact-friction conditions are enforced by a standard langrangian multipliers approach : these multipliers can be seen as the nodal forces appearing in the discretised numerical model due to the enforcement of the contact-friction conditions (2). An extended version (Ben Dhia, 2000 and 2001) for friction of the active constraint method developed for contact (Dumond, 1995) is applied for the resolution of the contact-friction problem at each time step. Although the original version of Dumond ensures the convergence of the algorithm by activating (gap between the solids violated) or deactivating (negative contact force applied by the slave component to the master component along an oriented direction going from the master to the slave contact surfaces) the contact conditions one by one, we chose to activate or deactivate the contact conditions by blocks.

The normal at the master surface is considered for the determination of the gap between the two components. Figure 1 shows a schematic view of the contact problem. In this study, the adhesion phenomena between the two components is not taken into account.

A Coulomb friction law is used for the mathematical representation of the friction, which implies that the tangential force depends linearly only on the normal force, and

cannot exceed a threshold value. The resolution of the friction problem is done by applying a prediction-correction (fixed point) method. It consists of solving, first of all, the contact problem, and then the friction problem for a fixed status of contacting nodes. Then the contact problem is checked again, and so on until convergence is reached (Ben Dhia, 2000 and 2001).

Approximate location of figure 1

At each time step, one has to verify the following system :

$$\begin{cases} u^{master} n^{master} + u^{slave} n^{slave} \le g \\ f_n^{slave/master} \le 0 \\ f_n^{slave/master} \left(u^{master} n^{master} + u^{slave} n^{slave} - g \right) = 0 \\ \left| f_t^{slave/master} \right| \le \mu \left| f_n^{slave/master} \right| \\ \dot{u}_t^{slave} - \dot{u}_t^{master} = \lambda f_t^{slave/master} \\ \lambda \left(\left| f_t^{slave/master} \right| - \mu \left| f_n^{slave/master} \right| \right) = 0 \\ \lambda \ge 0 \end{cases} \qquad (2)$$

Where the superscript denotes the component, master or slave, and the subscript denotes the direction : normal (n) or tangential (t).

Moreover we denote :

$f^{slave/master} = \left(f^{slave/master}.n \right) n + \left[f^{slave/master} - \left(f^{slave/master}.n \right) n \right] = f_n^{slave/master} n + f_t^{slave/master} t$:

the nodal force (equivalent lagrange multiplier) corresponding to the action of the slave component on the master component with a normal component along the direction of approach n defined below (when a point is non contacting then

$f_n^{slave/master} = f_t^{slave/master} = 0$),

u^{slave}, u^{master} : the displacement fields of the components depending on the superscript,

g : the oriented gap between the master and the slave surfaces,

n^{slave}, n^{master} : the normal vector (in practice related to the direction of approach) to the slave or master component depending on the superscript,

μ : the Coulomb friction coefficient.

λ : an unknown positive (sliding condition when contact and $\left|f_t^{slave/master}\right| = \mu\left|f_n^{slave/master}\right|$) or null (sticking condition when contact and $\left|f_t^{slave/master}\right| < \mu\left|f_n^{slave/master}\right|$) coefficient. In the discretised problem we never solve directly λ. We solve for $f_t^{slave/master}$ such that $\dot{u}_t^{slave} - \dot{u}_t^{master} = 0$ in case of sticking and

$f_t^{slave/master} = \mu\left|f_n^{slave/master}\right| \dfrac{\dot{u}_t^{slave} - \dot{u}_t^{master}}{\left|\dot{u}_t^{slave} - \dot{u}_t^{master}\right|}$ in case of sliding.

The first three relations of (2) correspond to the Signorini conditions of unilateral contact. The last four relations correspond to the Coulomb friction condition.

Different choice for the direction of approach n related to the normals n^{master} and n^{slave} are possible to determine the gap between impacting bodies. Indeed the normals n^{master} and n^{slave} are replaced in the previous system of equations by this direction of approach n in such a way that $n^{master} = n$ and $n^{slave} = -n$. One of the most common direction of approach for impacting solids is the normal to the master surface : $n = n^{master}$. Another one currently used is also $n = (n^{master} - n^{slave})/2$. We chose the first one in this study.

2.2 Formulation of the fluid load

At the nominal configuration, primary coolant circulates from the lower part to the upper part of the fuel assembly. Fluid loads consist of Archimedes principle of buoyancy ($F_{Archimedes}$) and forces induced by pressure losses, viscous friction, fluid pressure and lift force. They are located in three distinct zones : in the control rod drive mechanism ($F_{Mechanism}$), in the inner part of the control rod guide (F_{Stick}) and in the guide

thimble (F_{Guide}). In each zone different types of singularities may exist : section variation, bifurcation, holes for the passing fluid.

For the calculation of these fluid loads, the rod cluster control assembly and the guide are supposed to be straight. The fluid is supposed to be incompressible and viscous. Its density is supposed to be homogenous and constant. The fluid load is applied to the neutral fibre of the beam element representing the rod cluster and oriented vertically from the bottom to the top of the structure. It is evaluated at each time step, and it depends on the altitude of the rod.

The fluid loads are obtained by considering a weak fluid structure coupling. They are deduced from the conservation laws (mass conservation and energy conservation) in the annular fluid domain between the control rod and the guide. This methodology is applied at each singularity and along the guide for each zone defined previously.

A complete description of the fluid loads is presented in (Nhili, 2003).

3 Numerical modelling

A three dimensional numerical model of the rod cluster/guide system was carried out with a finite element approach with the Code_Aster®, finite element software, developed by the research and development mechanical engineering department of EDF. The rod cluster control assembly consists of many rods attached at their upper extremity to a spider, and of a cylindrical body for the control rod drive mechanism.

The fuel assembly is composed of fuel rods and guide thimbles in which the control rods pass through. The particularity of this structure is its dimensions. The guide thimble is about 4 m. The gap between the rod and the guide is very small (about 0.8 mm) and it becomes less than 0.2 mm at the dash pot (see figure 2). High pressurised water flows in this guide from its bottom to its top.

We assume the movement of the rods is in phase, and that they do not turn around their vertical axis. So, we model the rod cluster control assembly as an equivalent Euler Bernoulli beam with 850 elements. We also assume that the movement of the guide thimbles are in phase. We model the guide as two equivalent parallel stiff Kirchoff plates with 550 elements.

Then, we have a numerical model with 13500 degrees of freedom. The equivalence between the numerical model and the real structure is checked in terms of its mechanical behaviour. The difference between the numerical model and the real structure for the first two eigen frequencies is less than 2 %.

The displacement of the rod is large and supposed to be in an in plane vertical movement which we have to choose carefully when the guiding system is deflected. Fluid and mechanical loads are applied on the rod cluster. As mentioned before fluid loads consist of Archimedes principle of buoyancy and forces induced by pressure losses, viscous friction, fluid pressure and lift force. Mechanical loads are gravity, contact and friction forces.

Approximate location of figure 2

The figure 2 shows a schematic description of the model for straight, for C-shaped or for S-shaped guides.

The contact between the plate elements and the beam elements is taken into account. The choice of the normal direction for the evaluation of the gap between the two components is very important. Here, the direction of the normal is chosen as the normal to the plate element.

The friction force between the equivalent beam which represents the rod cluster control assembly and the equivalent plate which represents the guide is a vertical force applied directly to the neutral fibre of the beam. In fact, this friction force should be applied to

the external envelope of the rod, but due to the small radius of the rod, we applied it directly at the neutral fibre of the beam. We neglected the bending moment due to the radius of the beam.

The hydraulic loads are evaluated at each time step. They depend on the position (altitude) of the rod in the guide.

The differential equation of the movement (1) is solved by using the implicit integration Hilber–Hugues–Taylor method (Hilber, 1977). This regularization reduces the high frequency effect due to the non-linearity of the system.

The time step is chosen equal to 10^{-3} s. This time step respects the Courant condition (Courant, 1928). It is two times less than the time needed by the bending wave to cross adjacent nodes in the finite element model. The feasibility of this calculation is presented in (Andriambololona, 2005). The method was improved here by modifying the partitioning of the susceptible contact zone.

3.1 Resolution procedure

To obtain a bowed guide for the experimental set up, a lateral displacement is imposed at each grid. The values of these displacements correspond to a static boundary condition of the guide thimble MAC3S[2] methodology (Billerey, 2004). One can then obtain numerically the static deformation of the guide thimble which serves us for the meshing of a bowed guide.

The insertion force is very sensitive to the deflection of the guide. An adjustment to the deflection of the guide thimble obtained by MAC3S[2] is made in order to fit the calculated insertion force with the measured insertion force. This adjustment corresponds to an increased stiffness of the grid, which tends to make the guide almost vertical at the level of the grid (Bosselut, 2005).

In this study, we consider a straight and a bowed (C30 or S15-12) guide. They correspond to a C-shaped assembly bow and a S-shaped assembly bow respectively. The lateral displacement at the middle of the guide is equal to 30 mm for the C30 specimen. We mention that it is very small compared to the length of the fuel assembly, which is about 4 m.

For the S-shaped guide, the maximum lateral displacement at the lower part of the guide is equal to 15 mm, and at its upper part, the maximum lateral displacement is equal to 12 mm.

Two types of calculation can be simulated with the same model : the rod cluster insertion and the rod drop simulation. For the rod cluster insertion, the vertical displacement of the rod is imposed to be 1 m per minute and the fluid loads are neglected because the fluid is at rest. For the rod drop simulation, the rod cluster drops under its own weight from its withdrawn position, and all the loads described in the previous chapters are taken into account.

Approximate location of figure 3

The figure 3 summarizes the procedure for the simulation of the rod drop or the rod insertion.

3.2 Comparisons between experimental measurement and numerical calculations

Two types of numerical simulations are realized : the insertion and the drop of the rod cluster. Experimental measurements are obtained from a full-scale structure for the validation of the model. The full description of the measurement conditions and the experimental results obtained are described in (Collard, 1998).

The objective of the insertion test is to evaluate the friction force (integrated along the rod) due to the lateral displacement of the guide. It consists in imposing, at low speed,

the displacement of the control rod from its withdrawn position towards its inserted position. The results obtained are reaction force with respect to the altitude of the rod. The typical test results are the increase of the reaction force when the tip of the rod passes through a grid assembly distributed along the guide. An other typical result is the sharp increase of this reaction force when the tip of the rod is located in front of the dash pot. It is due to the simultaneous effect of a reduced gap and a lateral displacement of the guide at the dash pot. For an ideal straight guide, the reaction force should be equal to zero.

The insertion test may indicate the presence of a bowed guide. A none zero friction force implies that the guide or the rod is not straight. In this study, we assume that, initially, the rod is quite straight but that the guide may be bowed. For this test, the vertical displacement of the rod is slow and imposed to be 1 m per minute.

Figure 4 shows the comparison between the calculated and the measured resistance force for the insertion of a rod cluster with a 30 mm laterally deflected bowed guide as a function of the vertical displacement of the rod cluster. The Coulomb friction coefficient used to obtain this result is equal to 0.5. This value, chosen once for all, allows to have a good agreement between the calculated and the measured resistance force in all situations, and it is used for the calculation of the rod drop time. The numerical model can then simulates the mechanical behaviour of the system rod cluster/guide during the insertion. The insertion force analysis reveals that the resistance force depends closely on the deflection of the guide. The calculation is sensitive enough to localize a local abnormal deflection of the guide. It is indicated by an increase of the resistance force (at the grid level for example). The computer time needed for the numerical simulation of the insertion of the rod cluster is about 19 hours.

Approximate location of figure 4

The rod drop test is done to be sure of the effectiveness of the control system. It consists in letting the rod drop under its own weight. The measurement configuration presented here corresponds to a fluid flow rate of 284 m^3/h at a temperature of 50 °C. The results obtained are the evolution of the velocity of the rod with respect to time. The typical test result is the sharp decrease of the velocity when the tip of the rod arrives in front of the dash pot, due to the variation of the section of the guide at this location. It induces an increase of the fluid load which decelerates the drop of the rod. The behaviour of the evolution of the velocity depends on the shape of the guide.

Figure 5 and 6 show the results obtained respectively for the rod drop simulations of a C30 and a S15-12 guides. The result obtained with a straight guide is considered as the reference. They show the comparison between the estimated and the measured velocity as a function of time for a straight and a bowed guide. The effect of the hydraulic load is, in this case more important than the effect of the mechanical forces. If we only consider the gravity, the velocity increases with the time. Here, the fluid load is so important that it can oppose the vertical velocity of the rod. We can also see that if the guide is bowed, the friction force between the rod and the guide cannot be neglected. One can point out the difference between the velocity calculated with the C30 and the S15-12 guide.

Approximate location of figure 5

Approximate location of figure 6

Once more, we can see a good agreement between the numerical simulation and the measured data, excepted at the end of the drop for the calculated result with a straight guide, where we can observe an un-damped oscillation of the rod. It is probably due to the friction observed experimentally between the lower part of the rod cluster and the guide in the dashpot, due to a slight deviation of the rod during its oscillations, which cannot be simulated with a perfect straight rod cluster travelling in a straight guide. For a curved guide, this phenomenon is not observed.

The critical time for the rod drop is the duration of the drop. One has to measure or evaluate precisely the drop time : duration of the elapsed time between the initial configuration and the moment when the tip of the rod passes in front of the dashpot.

An other critical time is the elapsed time for the displacement of the tip of the rod from the entry into the dash-pot to its position when the velocity of the rod becomes null. These elapsed times must not exceed a limit value imposed by safety requirements.

The computer time needed for the numerical simulation of the rod drop is about 10 hours.

4 Conclusion

We present in this paper a method for the calculation of the insertion force of a rod cluster control assembly and the rod drop time. Fluid loads and friction forces are taken into account. A finite element model of the system is elaborated. We observe that the friction force cannot be neglected when the guide is bowed. The insertion force is very sensitive to the deflection of the guide.

The numerical model created here can be used to estimate the effect of an hypothetical deflection of the fuel assembly. So, the localisation of a geometrical defect on a guide can be achieved by analysing the drop velocity of the rod or by analysing the reaction force during an insertion simulation.

An improvement of the procedure is proposed in order to represent more accurately the 3D aspect of the contact at the tip of the rod and hopefully reduce the computer time due to the resolution of the contact friction problem. It consists in the resolution of the frictional contact problem by a continuous hybrid formulation proposed by Ben Dhia (Ben Dhia, 2002) coupled with the Arlequin approach (Ben Dhia, 1998, 2005) allowing

the use of local refined patches super-imposed and glued to the initial mesh. This topic is currently under investigation.

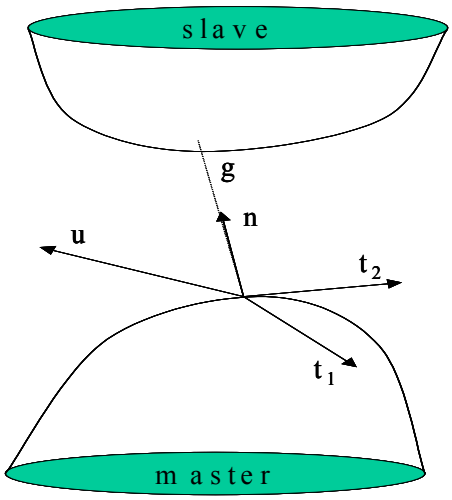

Figure 1 : Schematic view for the formulation of contact and friction between the master and the slave components.

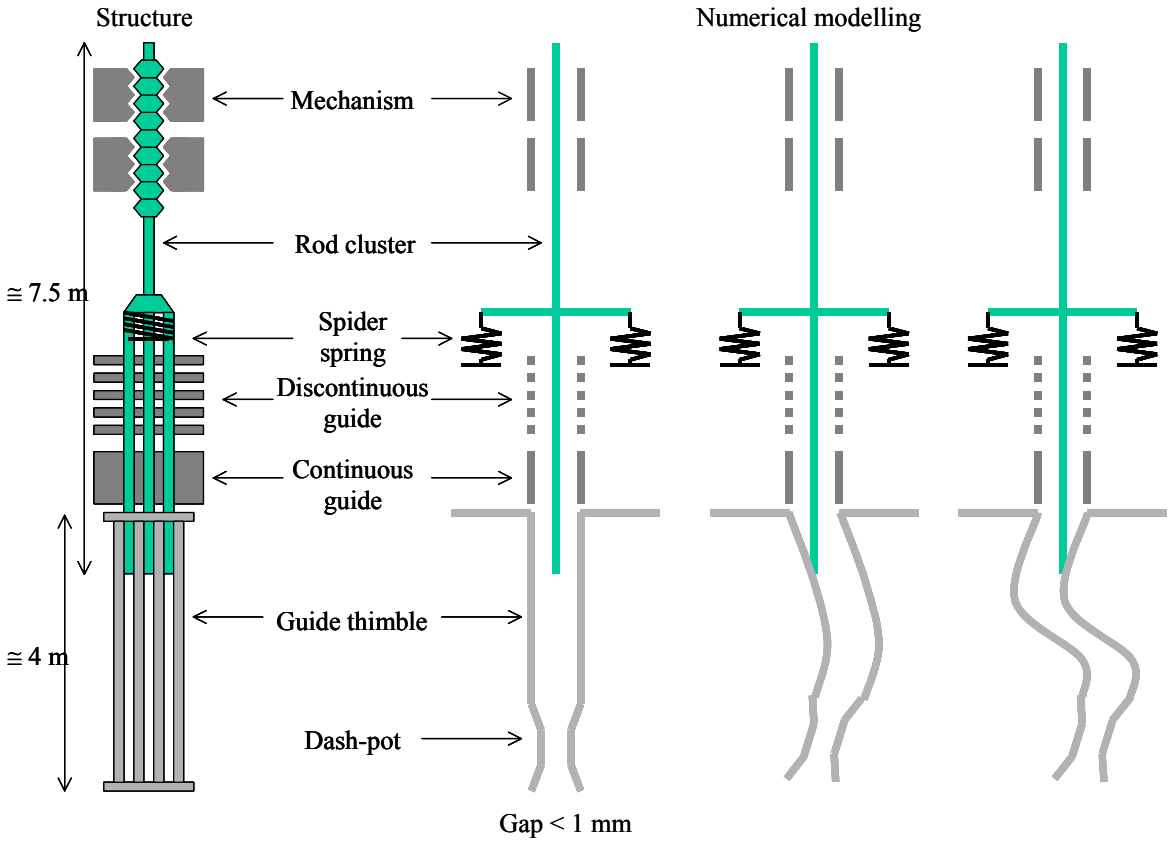

Figure 2 : Description and modelling of a rod cluster control assembly at its withdrawn position with a straight, a C-shaped and a S-shaped guide thimble. Choice of the in-plane observation plane.

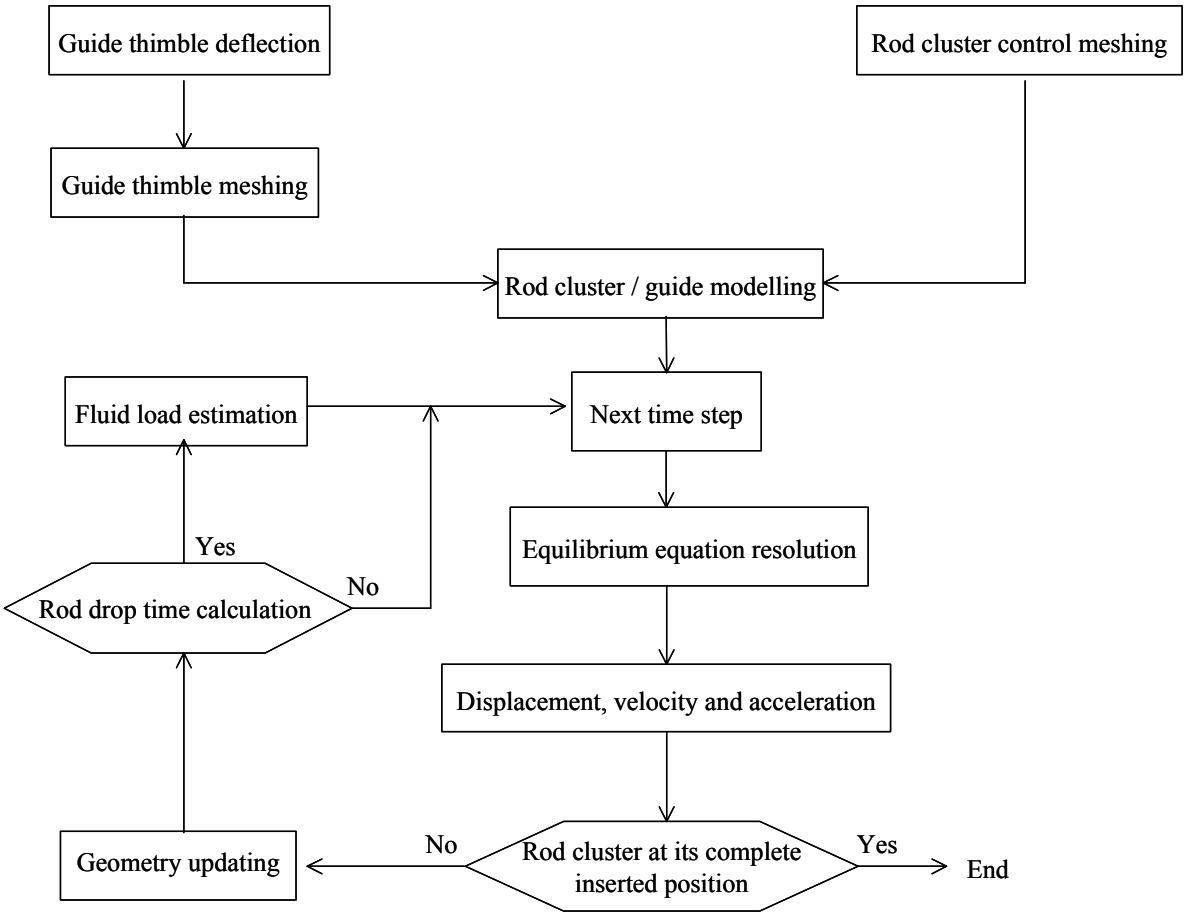

Figure 3 : Procedure for a numerical simulation of the rod drop or the rod insertion.

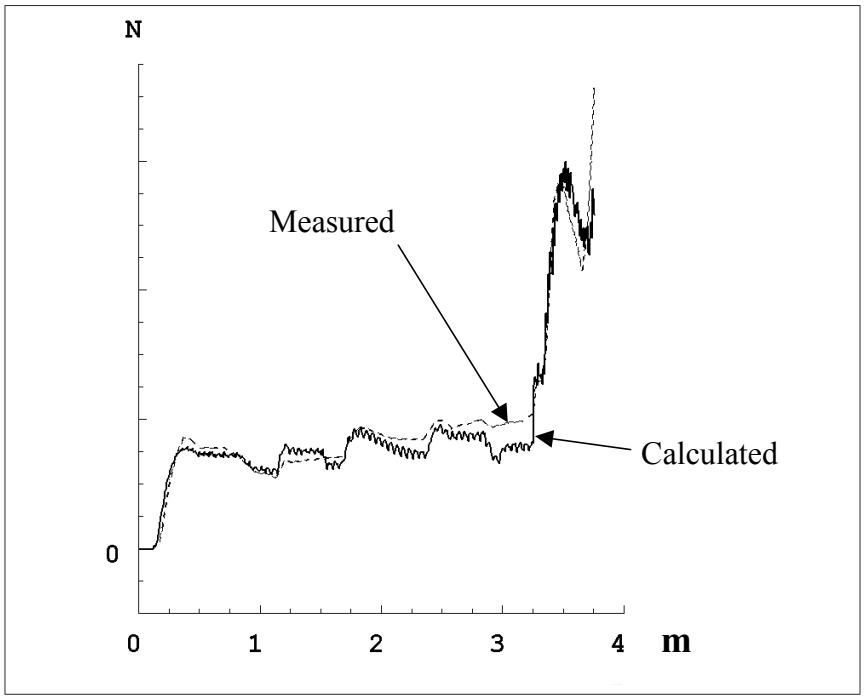

Figure 4 : Resistance force with respect to the altitude of the rod - Comparison between the calculated and the measured resistance force for the insertion of a rod cluster into a C-shaped guide thimble.

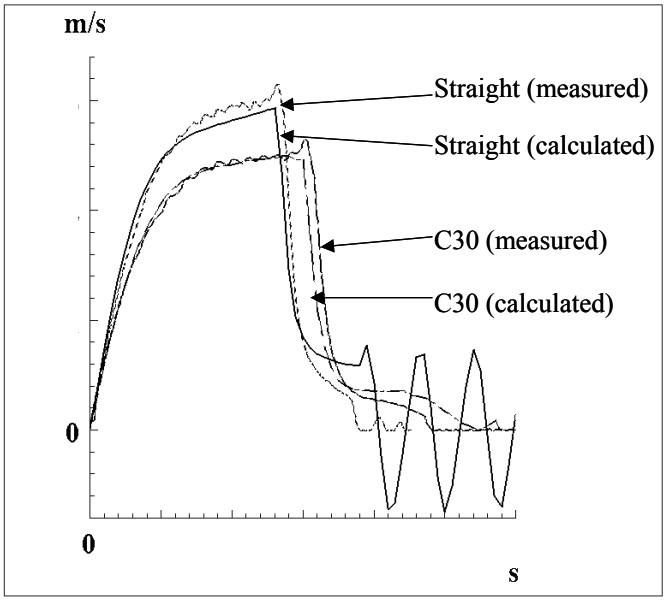

Figure 5 : Rod drop simulation : velocity with respect to time – A good agreement can be seen between the calculated and the measured data for a straight guide thimble and a C-shaped guide thimble, except for the end of the drop for the straight guide.

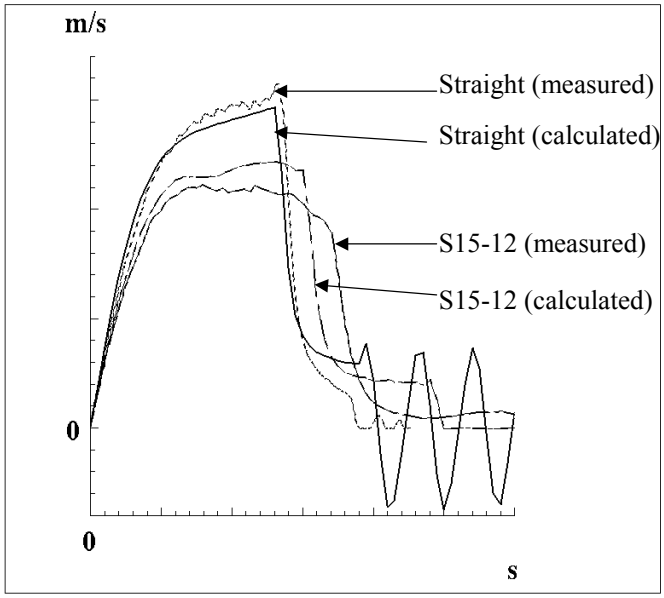

Figure 6 : Rod drop simulation : velocity with respect to time – Comparison between the calculated and the measured data for a straight guide thimble and a S-shaped guide thimble. The friction force cannot be neglected.

References

Andriambololona H., Bosselut D., Longatte E., 2005. Insertion of a slim structure into a channel – Simulations and parametric analysis. Proceedings of 6th International Conference on Structural Dynamics, Eurodyn 2005, pp. 1955-1959.

Aullo M., Rabenstein W. D., 2004. European Fuel Group experience on control rod insertion and grid to rod fretting. Technical meeting on Structural behaviour of fuel assemblies for water cooled reactors. IAEA-TECDOC-1454. pp. 147-163.

Ben Dhia H., 1998. Multi-scale mechanical problems : The Arlequin Method. C. R. Acad. Sci. Paris, Vol. 326, pp. 899-904.

Ben Dhia H., Massin P., 2000. 2D and 3D algorithms for frictional problems with small displacements. Proceedings of the European Congress on Computational Methods in Applied Sciences and Engineering, Barcelona, ECCOMAS 2000.

Ben Dhia H., Massin P., Tardieu N., Zarroug M., 2001. Différents algorithmes pour des problèmes de contact-frottement 2D et 3D en grands déplacements. Actes du cinquième colloque national en calcul des structures, Giens, France, pp. 1081-1088.

Ben Dhia H., Zarroug M., 2002. Hybrid frictional contact particles-in elements. Revue Européenne des Eléménts finis. Vol. 11 - n° 2-3-4, pp. 417-430.

Ben Dhia H., Rateau G., 2005. The Arlequin method as a flexible engineering design tool. International Journal for Numerical Methods in Engineering. Vol. 62, pp. 1442-1462.

Billerey A., 2004. Qualification du modèle MAC3-S² et détermination des caractéristiques mécaniques de l'assemblage de combustible irradié. EDF Septen report ENCNCA 04-0018 rév. A.

Bosselut D., 2005. Projet Sagrappe – Validation de la méthodologie Aster de calcul des forces d'insertion des grappes de commande. EDF report HT-62/04/023/A.

Collard B., 1998. Compte rendu des essais Cigare 900 MWE. Technical note DEC SECA/LHC 98/016.

Courant R., Friedrichs K., Lewy H., 1928. "Ueber die partiellen Differenzengleichungen der mathematischen Physik. Mathematische Annalen 100, pp. 32-74.

Dumond G., 1995. Algorithme de contraintes actives et contact unilateral sans frottement. Revue européenne des éléments finis. Vol. 4 - n°1, pp. 55-73.

Hilber H. M.,Hughes T. J. R., Taylor R. L., 1977. Improved numerical dissipation for time integration algorithms in structural dynamics. Earth. Eng. Struct. Dyn. 5, pp. 283-292.

Nhili R., Perotin L., 1996. Note de principe du logiciel de temps de chute des grappes de commande. EDF report HT-32/96/010/A.

Taliyan S. S., Roy D. P., Grover R. B., Manjit Singh and G. Govindarajan G., 1994. Dynamics of shut-off rod drop in a PHWR. Nuclear Engineering and Design, Volume 147, Issue 3, pp. 311-319.

Wang S. K., Chen Y. N., Chyou Y. P. and Yang T. T., 2003. Identification of damping mechanism of TRR-II reactor control rod during free fall insertion. Nuclear Engineering and Design, Volume 226, Issue 3, pp. 243-254.